3d Heat Transfer Analysis and Numerical Modeling of LENSTM Process for One End Stepped Cylindrical Wall by Using Stainless Steel 304

Chirag P. Patel[1], Prof. R. I. Patel[2]

[1,2](Department Of Mechanical Engineering, Government Engineering College, Dahod/ GTU, India

Abstract : Laser Engineered Net Shaping (LENS™) is a rapid-manufacturing process that involves complex thermal, mechanical, and metallurgical interactions. Due to process input parameter such as laser power , laser scanning velocity and feed rate, the effect on solidification of component to be produced must be understand. The finite element method (FEM) may be used to accurately model this process and solidification behavior by varying parameters. In this study the commercial FEM code ANSYS is used to predict the thermal histories, residual stresses, total deformation generated in One end stepped cylindrical wall and substrate of stainless steel 304. The computational results are compared with experimental measurements for validation.

Keywords: Laser engineering net shaping, FEM, Residual stresses, Total deformation, One end stepped Cylindrical wall, Element birth and death technique

I.   Introduction

Laser Engineered Net Shaping (LENS™) is a rapid manufacturing technology developed by Sandia National Laboratories (SNL) that combines features of powder injection and laser welding toward component fabrication. Several aspects of LENS™ are similar to those of single-step laser cladding. However, whereas laser cladding is primarily used to bond metallic coatings to the surfaces of parts that have already been produced with traditional methods[1], LENS™ involves the complete fabrication of three-dimensional, solid metallic components through layer by layer deposition of melted powder metal. In this process, a laser beam is directed onto the surface of a metallic substrate to create a molten pool. Powder metal is then propelled by an inert gas, such as argon or nitrogen through converging nozzles into the molten pool.

Depending upon the alignment of the nozzle focal point with respect to that of laser, then powder is then melted either mid-stream or as it enters the pool. As the laser source moves away, the molten material then quickly cools by conduction through the substrate, leaving a solidified deposit. The substrate is located on a 3 or 5-axis stage capable of translating in the X and Y-directions. Initially, a 3-D CAD model is created to represent the geometry of a desired component. The CAD model is then converted to a faceted geometry composed of multiple slices used to direct the movement of the X-Y stage where each slice represents a single layer of deposition. During the build, the powder-nozzle/laser/stage system first traces a 2-D outline of the cross section represented by each slice I the X-Y plane and then proceeds to fill this area with an operator-specified rastering pattern.
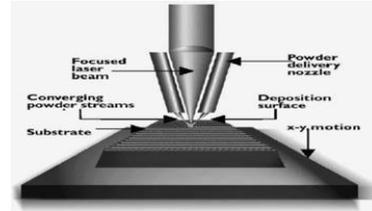
Figure 1 : Schematic Of LENS[TM] Deposition Process

The laser/nozzle assembly then ascends in the Z-direction so that the next layer can be added. This process is repeated for consecutive layers, until completion of the 3-D component [2]. This feature is illustrated schematically in Figure1.

II.   Literature Review

Keicher *et al.*[5] evaluated the effects of process parameters on multi-layer deposition of laser-melted powder Inconel® 625 in a process similar to both laser cladding and LENS[TM]. The group initially examined various parameters, including laser irradiance, stage translation speed, powder flow rate, powder particle size, and the size of each Z-directional increment   between layers and their effect on heat affected zone (HAZ) size generated during the build. The HAZ was defined in this study as the melted region below the surface of the substrate and was examined post-build via metallographic analysis. Khalen and Kar[10] performed an investigation into the effects of a several parameters on the resulting yield strength of AISI 304 stainless steel thin plates in process identical to LENS[TM] termed laser-aided direct rapid manufacturing (LADRM). This team sought to generate a range of input parameter values within which components with acceptable mechanical properties could be deposited. Their approach involved using the Buckingham Π-Theorem to express the process variables associated with heat transfer and powder mass flux in terms of 14 dimensionless parameters. Rangaswamy *et al.*[11,12] sought to experimentally measure residual stresses in LENS[TM] deposits using the neutron diffraction method, the details of which are discussed in next   Section The measurements were performed on LENS™-produced rectangular plates of AISI 316. The neutron data was collected at several points methodically distributed within the geometry of the samples, to provide a map of the stress distribution then calculated the axial components of residual stress through Hooke's law. Each stress component was then plotted against position within the plate, first, along the height (Z direction) on the sample vertical centerline, and next, along the width (Y-direction) on the plate horizontal centre line. Wang and Felicelli[15] next performed a parametric study similar to that done by Hofmeister *et al.*[8] to determine if the same trends in

cooling rates and thermal gradients were observable for different laser power. He repeated the previous simulation using five power intensity values, revealing that the temperature gradient at the edge of the molten pool increases substantially with laser power, while the cooling rate decreases. Neela and De[16] to study the effects of translation speed and laser power on the resulting temperature profiles using the general purpose FE package, ABAQUS® 6.6. The researchers used an element Activation/deactivation similar to those previously to model the deposition of a thin plate of AISI 316 with temperature-dependent thermal conductivity and specific heat according to a liner, and quadratic relation, respectively. Deus and Mazumder[17] attempted to predict the residual stresses resulting from a laser cladding deposition of C95600 copper alloy onto an AA333 aluminium alloy substrate. Since residual stresses would be generated by the heterogeneous

thermal expansions of the deposited and substrate materials, accurate stress calculations would also require accurate prediction of the temperature fields created during the build. Labudovic et al.[18] to predict residual stresses in a process identical to LENS™ termed the direct laser metal powder deposition process. A 3-D coupled model was implemented through the FE package ANSYS® for the deposition of a 50 mm x 20 mm x 10 mm thin plate of MONEL 400 onto a substrate of AISI 1006. The deposition was modelled with an ANSYS® element activation option similar to those already presented. Energy input density was modelled as a moving Gaussian distribution through the ANSYS® Parametric Design Language subroutine. The constitutive model was a temperature-dependent visco-plastic model, in which viscous effects were neglected by ignoring it the associated term in the equation of state.

III. CAD MODEL
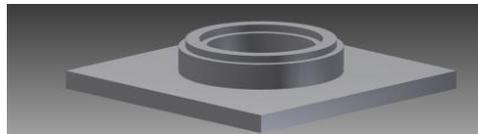
Figure 2 : Cad model for one end stepped cylindrical wall
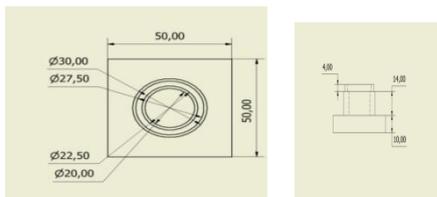
Figure 3 : Dimension for one end stepped cylindrical wall

The cylindrical wall model is created in the cylindrical coordinate system. x and y coordinates are defined as the radial and angular directions, respectively, while the z coordinate is defined in the vertical direction. A model for LENS process is built. As shown in Figure 3, Substrate : 50 x 50 x 10 mm. The example under consideration cylindrical wall upper cylinder has outer diameter 27.50 mm, inner diameter 22.50 mm and thickness 5 mm. the lower cylinder has outer diameter 30 mm, inner diameter 20 mm and thickness 10 mm. the total height H=18 mm. The 20 layers in the cylindrical wall height here each layer is assumed of equal 0.9 mm height .

IV. FINITE ELEMENT MODEL

The general purpose FE package ANSYS is used for both the thermal and stress analyses performed sequentially with an appropriate combination of elements. The main features of the 3D model are the moving heat input, the element birth-and-death technique, the heat loss, the temperature-dependent material properties, and the application of ANSYS parametric design language (APDL) to model the moving heat source and adaptive boundary conditions. The element types used in the thermal and structural analyses are SOLID70 and SOLID45, respectively. Both of them are the 8-noded brick elements that are compatible and can be automatically converted to each other during the solution process. The meshes used for

both simulations (thermal and structural) are the same. As shown in Figure 4, a total of 88919 nodes, and 44321 elements are generated to accomplish this simulation.
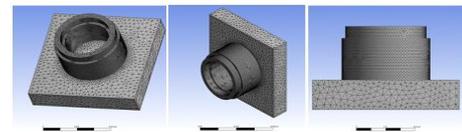
Figure 4: Meshing model for one end stepped cylindrical wall

V. THERMAL STRESS ANALYSIS

The first iteration in the solution procedure solves the system of equations at an assumed starting temperature (298 K), and the subsequent iterations use temperatures from previous iterations to calculate the thermal conductivity and specific heat matrices. The first born element is positioned onto the substrate with a set of initial and boundary conditions. For the subsequent elements, the model uses there results from the previous step as the initial condition for the birth of each new set of elements. This process is repeated for all the birthing events until the geometry is completed. After the structure has been built up the iterative process continues for some time required for the deposit to reach room temperature (the cooling sequence). Once the thermal simulation is done, the data regarding the temperature distribution in the buildup structure during the process is stored to a database. That data is used in the next step (structural analysis) as the only load that is applied as the body force. The structural simulation consists of the same steps during the building and cooling sequences as in the case of the thermal simulation. So, the temperature distribution scheme from some specific load step in the thermal analysis is applied to the corresponding load step in the structural analysis. It is

necessary to define the boundary conditions in the structural analysis to prevent a rigid body motion. Also, the intention is to allow substrate bending and reduce the influence of the rigid substrate on the stress development in the buildup as much as it possible. For these reasons, displacement of the substrate side surface, perpendicular to the wall depositing direction, is assumed to be zero.

VI. RESULT AND DISCUSSION

Since the cylindrical wall doesn't have free edges, the temperature distribution is different the higher average temperature is present along the circular path. Also at the start-end point of each layer, the laser beam dwells for some short time during the z-direction incremental movement. At that time , the heat input per distance moved along the wall length is increased, and the molten pool penetrates deeper into the previous deposit. Consequently the temperature is higher. As shown in figure 5 the inside surface lower cylinder has least deformation of value between 0.04075 to 0.034934mm.and the outer surface has maximum deformation of value between 0.052383 to 0.046566 mm. The all surface of lower cylinder and top of substrate has normal stress of value between 0.12365 to -0.076904 Mpa. and the side surface of substrate has normal stress of value between -1.8819 to -2.0824 Mpa.

As shown in figure 6 the top surface lower cylinder has maximum deformation of value between 0.077006 to 0.068877mm.and the bottom surface has intermediate deformation of value between 0.033668 to 0.02893

mm.and the side of substrate has minimum value of total deformation between 0.0052402 to 0.00050218 mm. The all surface of lower cylinder and all surface of substrate has normal stress of value between 153.54 and -53.541 Mpa. and maximum value of normal stress is 774.71 Mpa at contacting area of substrate and first layer of cylinder. As shown in figure 7 the top surface lower cylinder has maximum deformation of value between 0.086938 to 0.080775 mm. and the bottom surface has intermediate deformation of value between 0.056124 to 0.049961 mm. the top and all sides of substrate has minimum value of total deformation between 0.0068224 to 0.00065973 mm. The all surface of lower cylinder and all surface of substrate has normal stress of value between 74.086 to -137.53 Mpa. and maximum value of normal stress is 708.93 Mpa at contacting area of substrate and first layer of cylinder. As shown in figure 8 the top surface upper cylinder has maximum deformation of value between 0.090096 to 0.097008 mm. and the top and bottom surface of lower cylinder has intermediate deformation of value between 0.07627 to 0.034795 mm. The top and all sides of substrate has minimum value of total deformation between 0.014058 to 0.00023262 mm. The all surface of upper and lower cylinder and all surface of substrate has normal stress of value between 49.817 to -169.59 Mpa. and maximum value of normal stress is 708.03 Mpa at contacting area of substrate and first layer of cylinder.
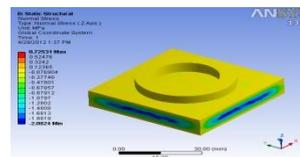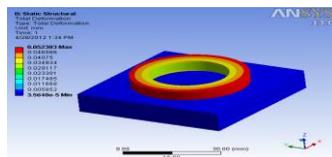
Figure 5 : Total deformation and Normal stress(σ_z) for 5 layers one end stepped cylindrical wall
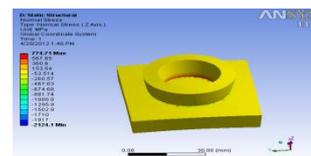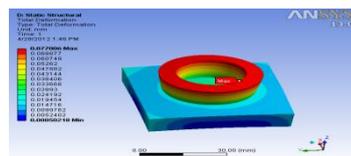
Figure 6 : Total deformation and Normal stress(σ_z) for 10 layers one end stepped cylindrical wall
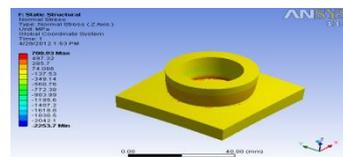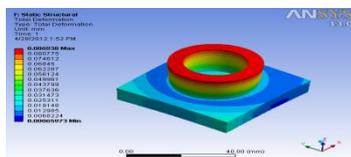
Figure 7 : Total deformation and Normal stress(σ_z) for 15 layers one end stepped cylindrical wall
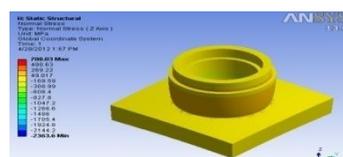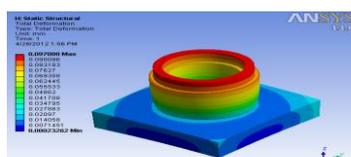
Figure 8 : Total deformation and Normal stress(σ_z) for 20 layers one end stepped cylindrical wall
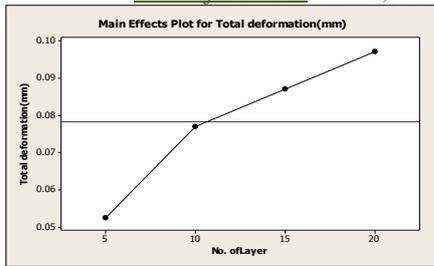
Figure 9: Graphical representation of total deformation for all layers
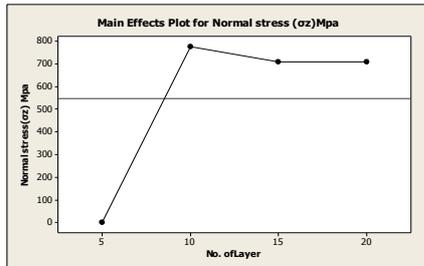
Figure 10: Graphical representation of Normal stress (σ_z) for all layers

As shown in figure 9 the cylindrical wall doesn't have free edges, the total deformation is different for 5, 10, 15, 20 layers. That difference means that the higher average deformation is present along the circular path which cause the higher deformation. Also at the start-end point of each layer, the laser beam dwells for some short time during the z-direction incremental movement. At that time, the heat input per distance moved along the wall length is increased, and the molten pool penetrates deeper into the previous deposit. Consequently the total deformation is higher, but it is s till lower than at the free edges because of the larger volume of the heat sink. Generally speaking, the one-directional deposited wall has stress values slightly higher than the cylindrical deposited wall which is expected according to lower temperature differences during deposition. Also, the high localized stress above the tensile strength observed at the corners. Because of the deposition strategy, the stress close to the free edges is not symmetric. The tensile stress is higher at the ending free edge. Some differences of the stress distribution between the cylindrical deposited walls can be observed at the free edges. Since, there is no laser beam reverse in the one-direction deposition strategy, the compressive stress in the z - direction has lower values. The lower residual stress is expected more in the cylindrical wall, which is proved by the analysis. The maximum residual stress is obtained at the bottom of the cylinder and the value is lower than the material yield strength. The stress distribution along at the inner surface is uniform except at the free end and the bottom of the cylinder where the stress behaviour is complex. If this result is compared with the stress distribution along the same line at the outer surf ace, that is also uniform, it is obvious that the axial stress σ_z and hoop stress σ y at the inner surface is tensile while the stress at the outer surface is compressive. The radial stress σ_x across the thickness of the wall change s the sign too, but it is much lower than the axial and hoop stress. As shown in figure 10 distribution of the stress causes a bending effect across the wall thickness.

VII.   CONCLUSION

The total deformation at the layers 5, 10, 15, 20 indicate that the pre-defined location is heated up when the laser beam passes over, and the negative peaks indicate that the pre-defined location cools down after the laser beam passes by, from the initial layer to subsequent layer depositions. At the first layer, the cooling rate decreases when the subsequent layers are deposited. After the third layer is deposited, the first layer still receives a maximum cooling rate. The maximum cooling rate for each pass decreases as more layers are deposited, which is due to the integrated heat of the substrate and previous layers. The maximum residual stress is obtained at the bottom of cylinder and contacting area of substrate and first cylindrical layer. The inner surface is tensile and the outer surface is compressive in terms of stress distribution and this distribution of stresses causes the bending effect across the thickness direction. The distribution of residual stress in cylindrical wall is uniform. There is no immediate crack observed maximum residual stress accumulated at the substrate center region. The stress in a cylindrical wall is seen to have maximum value at the top, with this value increasing with an increase in the number of layers in a wall, reaching a value of -298 Mpa at the top of a 20-layer wall.

VIII.   ACKNOWLEDGEMENTS

REFERENCES

[1] Vilar, R. J. Laser Cladding. Laser Appl. Vol 11. No 2. 1999. Pp. 64-79.

[2] Atwood, C., Griffith, M., Harwell, D., Reckaway, D., Ensz, M., Keicher, D., Schlienger, M., Romero, M., Oliver, M., Jeanette, F., Smugeresky, J. Laser Spray Fabrication for Net-Shape Rapid Product Realization LDRD. Sandia Report.1999.

[3] Sandia National Laboratories website.

[4] Griffith, M., Ensz, M., Puskar, J., Robino, C., Brooks, J., Philliber, J., Smurgeresky, J., Hofmeister, W. Understanding the microstructures and properties of components fabricated by laser engineered net shaping(LENS). Mat. Res. Soc. Symp. Proc. Vol 625. Warrendale, PA. 2000. Pp. 9-21.

[5] Keicher, D. Jellison, J., Schanwald, L., Romero, J. Towards a reliable laser spray powder deposition system through process characterization. 27th Int. Tech. Conf. Soc. Adv. Mat. Pro. Eng. Alburquerque, NM. 1995. Pp. 1009-1018.

[6] Hofmeister, W., Wert, M., Smurgeresky, J., Philliber, J., Griffith M., Ensz, M. Investigating solidification with the laser-engineering net shaping (LENS™) process. JOM-e.

[7] Hofmeister, W., Griffith, M., Ensz, M., Smurgeresky, J. Solidification in direct metal deposition by LENS processing. JOM. Vol.53. No 9. 2001. Pp. 30-34.

[8] Hofmeister, W., MacCalum, D., Knorovsky, G. Video monitoring and control of the LENS process. American Welding Society 9th International Conference of Computer Technology in Welding. Detroit, MI. 1998. Pp. 187–196.

[9] Smugeresky, J., Keicher, D., Romero, J., Griffith, M., Harwell, L. Laser engineered net shaping (LENSTM) process: optimization of surface finish and microstructural properties Proc. of the World Congress on Powder Metallurgy and Particulate Materials. Princeton, NJ. 1997. Part 21.

[10] Kahlen, F.-J., Kar, A. J. Tensile strengths for laser-fabricated parts and similarity parameters for rapid manufacturing. Manuf. Sci. Eng. Vol 123. No 1. 2001. Pp. 38-44.

[11] Rangaswamy, P., Holden, T., Rogge, R., Griffith, L. J. Residual stresses in components formed by the laser-engineered net shaping (LENS®) process. Strain Analysis. Vol 38. No 6. 2003. Pp. 519-528.

[12] Rangaswamy, P. Griffith, M., Prime, M., Holden, T., Rogge, R., Edwards, J., Sebring, R. Residual stresses in LENS® components using neutron diffraction and contour method.Mat. Sci. Eng. A. Vol 399. 2005. Pp. 72-83.

[13] Riqing, Y., Smugeresky, J., Zheng, B., Zhou, Y., Lavernia, E. Numerical modeling of the thermal behavior during the LENS® process. Mat. Sci. Eng. A. Vol 428. 2006. Pp. 47-53.

[14] Lindgren, L.-E. Finite element modeling and simulation of welding part : increased complexity. Journal of Thermal Stresses. Vol 24. 2001. Pp. 195-231.

[15] Wang, L., Felicelli, S. Analysis of thermal phenomena in LENS™ deposition. Mater. Sci. Eng. A. Vol 435-436. 2006. Pp. 625-631.

[16] Neela, V., De, A. Numerical modeling of LENS™ process using special element features.2007 Abaqus India Regional Users' Meeting. 2007.

[17] Deus, A., Mazumder, J. Two-dimensional thermo-mechanical finite element model for laser cladding. Proc. ICALEO. Duley, W., Shibata, K., Poprawe, R., eds. Orlando, FL. Laser Institute of America. 1996. Pp. B/174-B/183.

[18] Labudovic, M., Hu, D., Kovacevic, R. A three dimensional model for direct laser metal powder deposition and rapid prototyping.J. Mat. Sci. Vol 38. 2003. Pp. 35-49.